Golub, M.; Lott, D.; Haramus, V.M.; Laipple, D.; Stoermer, M.; Watkins, E.B.; Schreyer, A.; Willumeit-Roemer, R.:

Neutron study of phospholipids 1-palmitoyl-2-oleoyl-sn-glycero-3-phospho-ethanolamine spray coating on titanium implants

In: Biointerphases (2015) American Vacuum Society

DOI: 10.1116/1.4938556

Neutron Study of Phospholipids 1-palmitoyl-2-oleoyl-sn-glycero-3-phospho-ethanolamine Spray Coating on Titanium Implants

Running title: POPE spray coating

Running Authors: Golub et al.

Maksym Golub [a)]

University Joseph Fourier, Institute of Structural Biology, 71 Avenue des Martyrs, 38000 Grenoble, France.

Dieter Lott

Institute of Materials Research, Helmholtz-Zentrum Geesthacht Zentrum für Material- und Küstenforschung (HZG), Max Plank 1, 21502 Geesthacht, Germany

Vasil M. Garamus

Institute of Materials Research, Helmholtz-Zentrum Geesthacht Zentrum für Material- und Küstenforschung (HZG), Max Plank str. 1, 21502 Geesthacht, Germany

Daniel Laipple

Institute of Materials Research, Helmholtz-Zentrum Geesthacht Zentrum für Material- und Küstenforschung (HZG), Max Plank str. 1, 21502 Geesthacht, Germany

Michael Stoermer

Institute of Materials Research, Helmholtz-Zentrum Geesthacht Zentrum für Material- und Küstenforschung (HZG), Max Plank str. 1, 21502 Geesthacht, Germany

Erik B. Watkins

MPA-11, Los Alamos National Laboratory, Los Alamos, United States

Andreas Schreyer

Institute of Materials Research, Helmholtz-Zentrum Geesthacht Zentrum für Material- und Küstenforschung (HZG), Max Plank str. 1, 21502 Geesthacht, Germany

Regine Willumeit-Römer

Institute of Materials Research, Helmholtz-Zentrum Geesthacht Zentrum für Material- und Küstenforschung (HZG), Max Plank str. 1, 21502 Geesthacht, Germany

[a)]Electronic mail: maksym.golub@hotmail.com

Permanent implants made from titanium are widely used and successfully implemented in medicine to address problems related to orthopedic and oral disorders. However, implants that interact in all cases optimally and durably with bone tissue have yet to be developed. Here we suggest a POPE (phospholipids 1-palmitoyl-2-oleoyl-sn-glycero-3-phospho-ethanolamine) lipid coating to partially mimic the biological cell membrane.

To improve the homogeneity of the POPE distribution on the metal surface, the lipids are applied by spray coating. It is shown that the spray coating leads to two types of multilamellar POPE structures. Our experimental results demonstrate that these coatings are stable in a liquid environment in the range of physiological temperatures due to the unique interbilayer interaction of POPE lipids. Additionally, the interaction of the POPE multilayer structure with Human Serum Albumin (HSA) is considered. A simultaneous analysis of the specular and off-specular data provides structural information necessary to assess the quality of the coating for future applications.

I. INTRODUCTION

The application of medical implants as secure solutions for problems with the musculoskeletal system is well established. Still, due to the increased lifespan, changing lifestyles and, of course, improved implant technology [1] the demands especially related to durability have grown constantly. Diseases and problems caused by damaged or diseased bone tissue represent an annual cost that now exceeds 40 billion Euros worldwide [2]. Furthermore, the rapid increase in the number of elderly and multimorbid people [3] requires that tissues and organs endure longer and are also able to perform in compromised health conditions [4]. Modern science has provided novel insights into the biological mechanisms responsible for bone healing. These achievements currently push forward the development of implants with “smart” implant surfaces to interact optimally

with the bone tissue. In this way, implants can contribute to regaining health and improving quality of life for much longer periods of time than currently possible.

The materials that are implanted in bone tissue are required to be non-toxic, non-immunogenic, non-thrombogenic and non-carcinogenic [5]. In this respect, titanium and its alloys have become preferred materials due to their good biocompatibility [6].

Several attempts have been made to develop new implant surface modifications which may prolong the lifespan of a permanent implant and ensure quicker and more stable implant incorporation, therefore giving patients shorter recovery time. To obtain biologically active materials that provide biological cues for tissue regeneration, various coatings are applied. Besides hydroxyqpatite, proteins or short sequences of proteins (RGD-peptides) are used to funtionalize the surface [7]. Antimicrobial coatings are produced by using silver or copper coatings. Phospholipid coatings on titanium surfaces have been intensively studied in terms of adhesion, proliferation and differentiation of human bone derived cells (HBDC) [8-11], human chondrocytes and human mesenchymal stem cells, and of macrophage stimulation [12-14]. They proved to be a positive factor for cell-implant interactions.

So far the lipid coatings were mostly adsorptive which seems to indicate a very instable surface. In addition, POPE (phospholipids 1-palmitoyl-2-oleoyl-sn-glycero-3-phospho-ethanolamine) coatings are not distributed homogenously over the metal surface since titanium attracts neither methanol nor chloroform. However, the stability of the coating is sufficient because it keeps cells attached to a metal surface over weeks and stimulates osteogenic differentiation [15].

The main objects of this investigation are the determination of the structure and stability of POPE multilayers on a titanium surface i. e., titanium oxide and their alteration upon exposure to water and growth medium containing Human Serum Albumin (HSA), conditions that favor cell adhesion. The stability of the POPE multilayer structure at physiological temperatures under the POPE phase transition temperature is an important issue which is considered in this work. The study of the structure of the multilayer, including the structure normal as well as parallel to the surface, will facilitate the identification of key parameters to understand the interaction between cells and lipid-coated implants.

The selected protein is an important blood protein for which the molecular dimensions are well known [16]. Crystallographic data suggest that the quaternary structure of HSA is heart-shaped (see Fig. 1) with a width of 82 Å, a maximum dimension from the apex of the heart to the end of the domains on each side of 83 and 70 Å, respectively, and a depth of approximately 30 Å [17].

FIG. 1 HSA molecule (PDB code 1E7H [18]).

In this work neutron scattering techniques are applied for the investigation of lipid coatings on a titanium surface under different environmental conditions. This method allows to probe structure and interaction of lipid bilayers with membrane active molecules such as proteins [19] due to different scattering contrast. In addition, it is possible to study the lateral structure of the bilayers as well as the averaged scattering length density profile in the z direction. However, structural studies of biomembranes are difficult, even for pure lipid bilayers, because of thermal fluctuations [20]. Biologically relevant lipid membrane multilayers on the surface are still fluidic resulting in a decreased number of diffraction peaks needed for crystallographic analysis when the lipid layers are fully hydrated.

II. EXPERIMENTAL SET UP AND METHODOLOGY

A. Substrate preparation

In order to mimic a Ti – implant surface and to have a roughness sufficient for reflectometry studies, titanium (99.7% pure, PureTech, New York, NY, USA) was deposited on two initially identical silicon crystals (8 x 5 x 1 cm) with a polished surface provided by Siltronix Archamps Technopole (Archamps, France). Thus, two Ti-coated Si crystals (substrates) with different thickness of the titanium layer of 37nm and 100 nm were prepared, allowing a more precise investigation of the POPE lipid structure. All depositions were performed at the Helmholtz Zentrum Geesthacht (HZG) using a magnetron sputter deposition chamber capable of handling large substrates [21] according to the procedure described in [22].

B. Lipid Deposition

In order to perform a complete POPE coating of this titanium surface an air brush (Hansa World Of Airbrush Marketing and Sales GmbH, Osteinbek, Germany) was used to spread lipids evenly. The air brush was connected to a nitrogen steam at pressure of 0.5 bar, thus, 2mL of the POPE solvent solution with the lipid concentration of 1 mmol POPE per 1 L solvent (20% methanol and 80% chloroform) were distributed over 8 x 5 cm^2; the average deposition time was about 1 minute.

POPE lipids are deposited as an aerosol so that the drops of methanol and chloroform evaporate before they start to move on the surface, due to the hydrophobic force between the titanium dioxide and the solvent. The main advantages of the spray deposition is that the spray coating might be the easiest way to coat a real implant with a complicated shape, for which other methods such as Langmuir-Blodgett deposition or spin coating are difficult to apply. The easily applicable drop- or dip- coating methods lead to an extremely uneven distribution of the POPE lipids over the surface and is not suitable either for reflectivity studies.

C. Scanning Electron Microscope (SEM)

Scanning Electron Microscope (SEM) measurements were done by an Auriga (Zeiss, Oberkochen, Germany). SEM-images are taken at 1-6 kV accelerating voltage using either the SE2 detector or the InLens detector in order to gain topographical and surface contrast.

The POPE layers were analyzed by Energy Dispersive X-ray Spectroscopy (EDS) using the EDS device Apollo XP from EDAX (Ametek GmbH, Wiesbaden, Germany) attached to the Auriga. Due to a high EDS counting rate SEM aperture of 120µm diameter had been used in High Current mode. EDS mapping was realized over 7 regions of interest in the respective EDS spectrum, i.e. Ti, Al, Nb, C, P, O, and Si, to identify the element distribution on the surface. For every image about 512 frames with a resolution of 512 x 400 points were mapped. At each point a dwell time of 200 µs was applied. During EDS - mapping drift correction was applied to enhance quality.

The cross beam workstation Auriga was furthermore equipped with the focused ion beam (FIB) device Canion from Orsay physics (Fuveau, France), using gallium. To assess the thickness of the POPE coating in an alternative way, cross sections of POPE layers were prepared by FIB milling at 30 keV using a current of 2 nA. Observation of the morphology of the cross-section was performed directly after cutting at 1 keV. An additional EDS mapping on this cross section was done at 5 keV.

D. Neutron Experiments

The neutron reflectivity measurements were performed on the time-of-flight reflectometer Figaro (ILL, France). The experiments were carried out using the standard Figaro solid-liquid interface sample cells [23]. Contrast variation experiment was applied by exchanging H_2O and D_2O buffer solutions. The temperature structure dependence was studied in the range from 20 °C to 42 °C. To discover structural changes of POPE under different environmental conditions, D_2O-based growth medium with and without the addition of deuterated HSA protein was sequentially injected into the sample cell. The deuterated protein was kindly provided by the D-Lab of the ILL, Grenoble. The protein concentration in the growth medium was 5mg/mL.

Two incident angles (0.624 and 3.78 degrees) were used to enable measurements of the reflectivity up to 0.3 $Å^{-1}$ in Q_z using wavelengths of the incoming beam in the range from 2 - 30 Å. The wavelength resolution for this measurement was kept constant at 4.2% by the applied chopper system settings. The divergence of the incident angle was less than 2%, resulting into an overall dQ_z/Q_z resolution of 4.7%. For data collection, a 2D Helium-3 detector was used with an active area of 500 x 250 mm^2 and a resolution of 2 x 7 mm^2. A more detailed description of the Figaro reflectometer can be found elsewhere [23]. For the data treatment, the raw data were converted into Q_x-Q_z maps and the gravity effect on the neutrons due to horizontal sample geometry was taken into account [24, 25]. The analysis of the POPE multilayer structure in the z direction was done by integrating a cut over the Q_x-Q_z maps along Q_z around Q_x=0 $Å^{-1}$ (ΔQ_x = ±0.00015 $Å^{-1}$), separating the specular region. The information about the in-plane structure of POPE coating was extracted from the cut over the Q_x-Q_z maps along Q_x at constant Q_z values.

For the data analysis, a semi-kinematic approximation was used. The reflectivity of a rough interface can be expressed as follows [26]:

$$R(Q_z) = R_F(Q_z)\left|\frac{1}{\rho_s}\int_{-\infty}^{\infty}\frac{d\rho(z)}{dz}\exp[iQ_z z]dz\right|^2 \qquad 1$$

where R_F is the so-called the Fresnel reflectivity [26], ρ(z) is the scattering length density (SLD) profile along the normal direction (Z) of the surface and ρ_s is the total difference in the SLD between the two adjoining media (silicon and water or silicon and air in this experiment).

To fit the reflectivity data, we applied a model of two incoherent contributions. We had to consider that for one of two contributions the absorption was not negligible. Thus, the reflectivity in this case can be approximated by the formula (2):

$$R(Q_z) = R_1(Q_z) + \frac{(1-R_1(Q_z))^2 R_2(Q_z)A(D)}{1-R_1(Q_z)R_2(Q_z)A(D)} \qquad 2$$

Where $A(D) = Exp\left[-\frac{2*\mathrm{Im}\,SLD*D}{Sin(\theta_{in})}\right]$, $R_1(Q_z)$ is the reflectivity from the TiO_2/lipid interface and $R_2(Q_z)$ is the reflectivity from the lipid/D_2O interface. D is the thickness of

the POPE coating, Im SLD is the linear absorption coefficient, and θ_{in} is the incident angle of the neutron beam.

The Motofit program [27], based on the Parratt recursion formula [28], is applied to find the best model description of the perpendicular density profile by considering the least-squares fitting between the simulated and experimental neutron reflectivity data. For a non-Gaussian roughness, the scattering length density profile was approximated by slicing the interface into thin slabs of continuously varying scattering length densities [29].

III. RESULTS AND DISCUSSION

A. SEM pre-characterization

The spray-coated titanium surface was probed by SEM (see Fig. 2A). The images indicate that the surface was coated very inhomogeneously with many POPE "islands", with an average size of 20 μm.

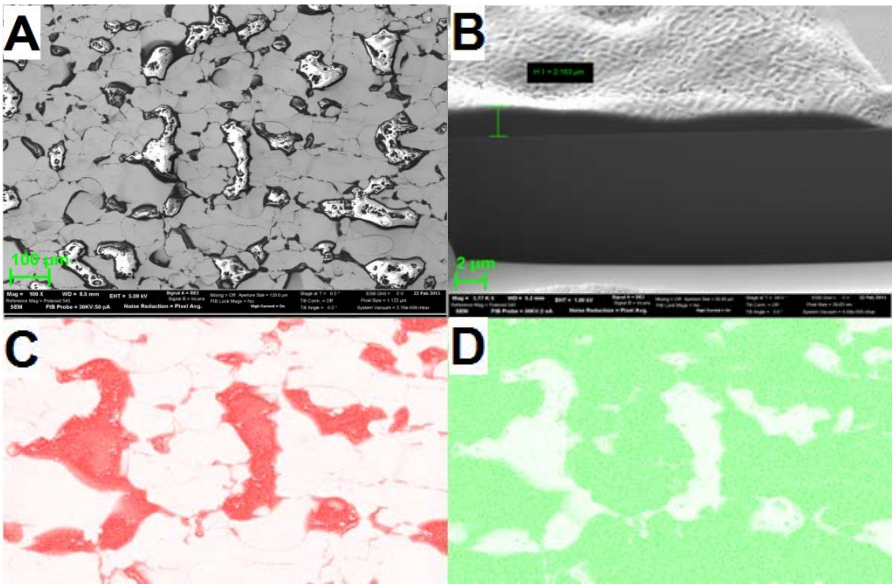

FIG. 2 SEM images of the spray-coated Ti surface: overview picture (A); cut of the surface (B); mapping of the chemical composition: the red color corresponds to carbon (C), and the green color corresponds to titanium (D).

To evaluate the thickness of these islands, the spray-coated sample was cut with a Ga beam with an energy of 30 kV (Fig. 2B). This cut revealed that the thickness of the

islands was in the order of 1-2 µm, which corresponds to approximately ~250 lipid bilayers. The mapping of the chemical composition demonstrated that most of the POPE lipids were concentrated on these “islands”; however, the areas between the islands were also coated with POPE (light red colour indicates to presence of C, lipid), which is an important result in respect to implant modifications.

B. Neutron reflectivity experiments to study the overall structure of the coating

In the following, the spray-coating was investigated in a liquid environment by neutron reflectivity. The two critical angles can be resolved for the measurement of the POPE spray coating against D_2O (see the green curve in Fig. 3). The observed decrease in intensity can be explained by the attenuation of the beam which completely penetrates the thick POPE coating. Such a decrease has been reported in literature by Zarbakhch [33] investigating a 1-2 µm thick oil layers placed in between a silicon crystal and a D_2O interface by neutron reflectivity[30].

To fit the reflectivity data from Fig. 3, we applied a model of two incoherent contributions. The assumed model is based on the SEM images displaying two types of POPE coating (thick and thin coating) on the titanium surface. In the case of the thin POPE coating, the reflectivity curve has the same critical edge as that one for the Ti coated Si-crystal (see the orange line in Fig. 3). For the thick POPE coating (see the cyan curve in Fig. 3), the absorption is not negligible. From the analysis of the decrease in the intensity at the critical edge, the thickness and the linear absorption coefficient can be evaluated. The calculations revealed that the Im SLD is approximately 1-3 x 10^{-8} $Å^{-1}$. Such a ImSLD value is in the range of previously obtained values for thick oil layers [17, 30], with a chemical composition that contains mostly CH_2 and a density of approximately 0.77 g/mL. The thickness of the thick coating was determined to be approximately 2 ± 1 µm, being in good agreement with the SEM results.

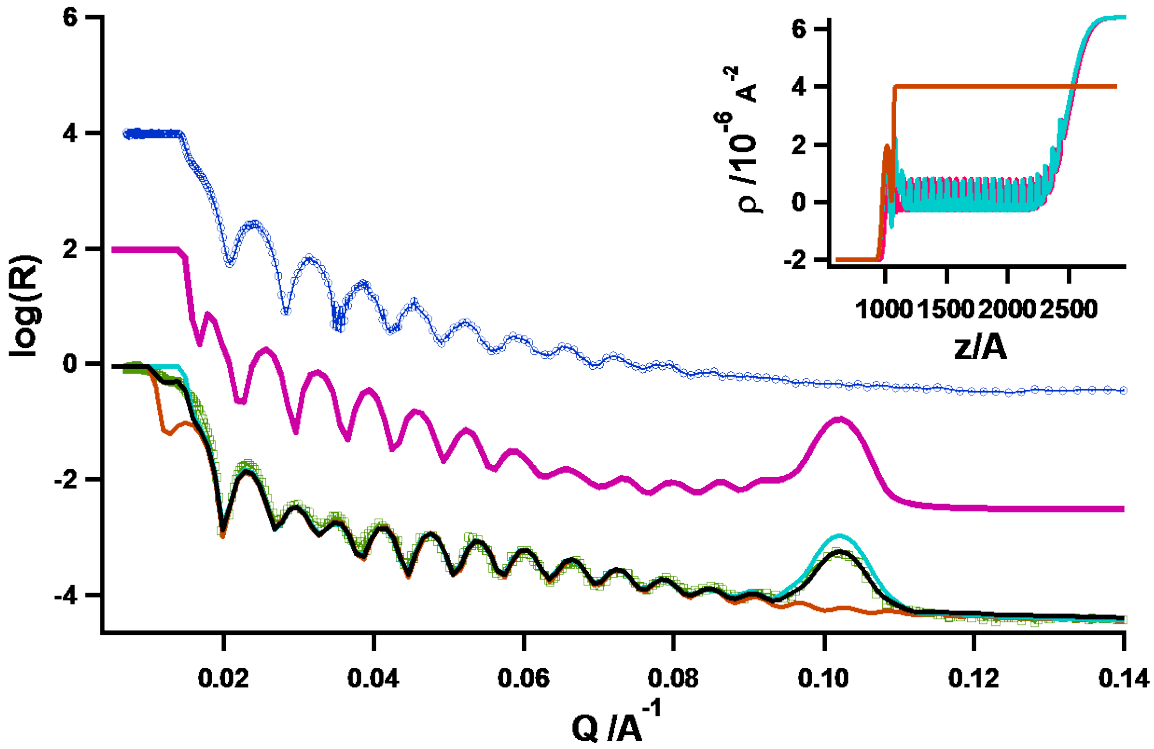

FIG. 3 Neutron specular reflectivity curves measured against D_2O. The blue circles correspond to the substrate (Ti coated Si-crystal). The violet solid line is the modeled reflectivity curve, which reveals the case of 40 POPE bilayers attached to the substrate. The green squares represent the real measured curve of the POPE coated substrate at 20° C. The cyan and orange solid lines correspond to the modeled specular reflectivity curves of the thin coating and thick coating, respectively. The black curve reveals the final fit within the incoherent model. The corresponding SLD profiles are given in the upper right corner.

Table 1. Neutron scattering length density (SLD) profile of the POPE coated substrate at 20° C.[1]

Sample	Material	Thickness, Å	SLD, 10^{-6} Å^{-2}	Roughness, Å
Ti coated Si-crystal	Si	None	2	None
	SiO_2	40	3.4	8
	Ti	985	-1.96	20
	TiO_2	35	2.4	20
Supported POPE bilayer	Head region	12	3±0.5	9
	Tail region	37	-0.3±0.5	15
	Head region	12	3±0.5	9
	Transition layer	80±20	-0.3±0.5	80±20
POPE thin coating				
Lipid Multilayer structure 40 repetitions	Water layer	6±2	1.3±1	5±3
	Head group	6±3	0.5±0.5	8±3
	Tail group	36.7±3	-0.3±0.5	15±6
	Head group	6±3	0.5±0.8	10±4
	Water layer	6±2	1.3±1	5±3
POPE thick coating				
Disordered POPE bilayers	Disordered POPE bilayers	20000±5000	4±1	8±3

The comparison of the reflectivity curves of the substrate (Ti coated Si-crystal) and the POPE spray coated substrate (see the blue curve and the green curve in Fig. 3) reveals that the shape of the higher frequency oscillations of the reflectivity curve, that are related to the Ti layer and TiO_2, has changed. The positions of the oscillation have shifted to smaller Q_z values indicating the attachment of an additional layer onto the

[1]The fitting parameters for the titanium crystal were taken without modification from the analysis of the reflectivity curve measured from the uncoated crystal s.
The SLD profile from the table is equivalent to the SLD profile obtained by the slicing fit.

surface. Moreover, the reflectivity curve of the spray-coated substrate contains a rapid decrease of the oscillation amplitude, the so-called beating point [29, 31], at Q_z position 0.035 $Å^{-1}$. From the position of the beating point, it is possible to determine that the thickness of the additional coating is 55-60 Å, which corresponds well with the thickness of one POPE bilayer. The shift and the corresponding beating point were observed independently from the two substrates with different thicknesses of the titanium layers. Therefore, we can conclude that in both cases one POPE bilayer must be well attached to the substrate and, at the same time, this bilayer is separated from the multilayer structure placed on the top. The final fit is presented in Fig. 3 as a superposition of the two model reflectivity curves calculated separately for the two types of POPE coatings.

C. Neutron reflectivity experiments to study the temperature sensitivity of the POPE coating

In a next step, the temperature behavior of the spray-coated sample was investigated from 20° C to 42° C. As shown in Fig. 4, the shape and positions of the oscillations remain unaffected for all measured temperatures, while the Bragg peak shifts to higher Q_z as the temperature increases. At 25° C, the POPE lipid undergoes a phase transition from the gel phase to the liquid crystalline phase due to the melting of the hydrocarbon region of the bilayers. The effect of the phase transition is evident in the green specular reflectivity curve in Fig. 4 with the emergence of a second Bragg peak indicating that both phases are present in the POPE multilayer. The peak position shows reversible changes at decreasing of T.

For each applied temperature, the position of the Bragg peak can be fitted by a Lorentzian function to obtain the temperature dependence of the POPE d-spacing (see Fig. 5). After the phase transition temperature, the d-spacing of the POPE bilayers changes linearly with temperature.

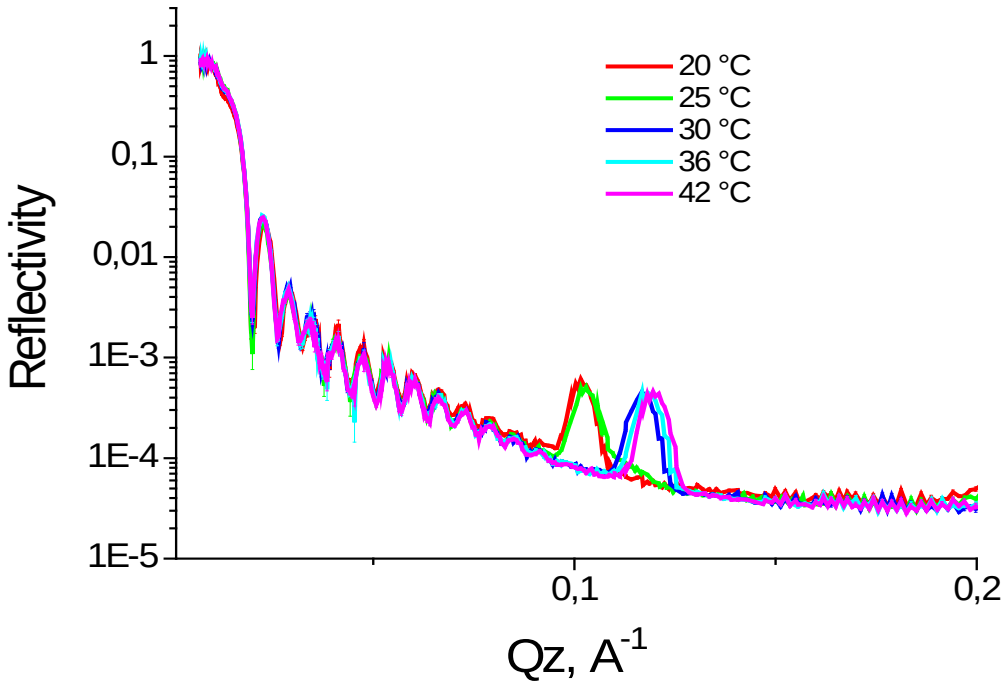

FIG. 4 Neutron reflectivity curves – the temperature behavior of POPE bilayers

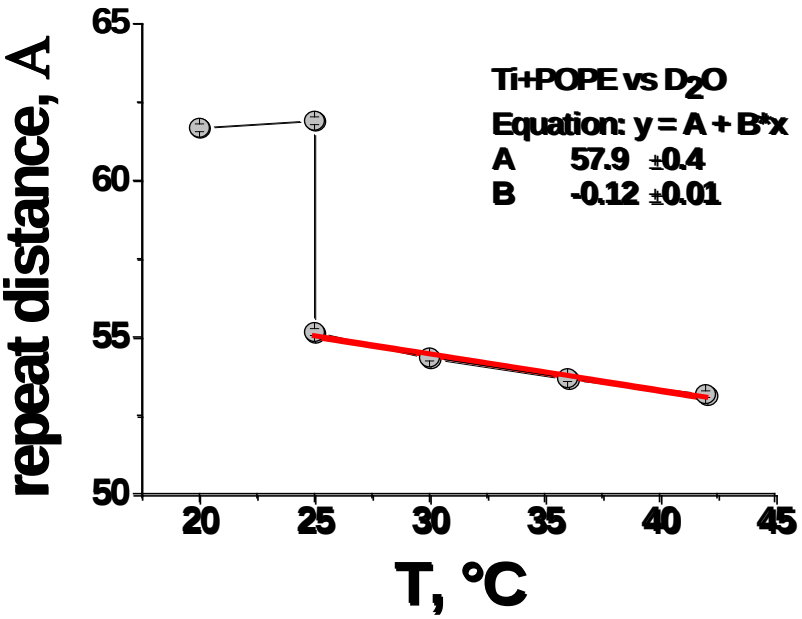

FIG. 5 Temperature behavior of the Bragg peak position: 1) Green dots correspond to the d-spacing of the POPE bilayer at different temperatures; 2) The red line – linear fit.

D. Neutron reflectivity experiments to study the influence of proteins on the coating

When this lipid coating is studied in cell culture, it is subjected to interactions with a solution of complex molecules. Here, we chose proteins as the most important class of molecules that come in contact with an implant surface. Thus would like to answer the question if protein adhesion on a lipid coating is possible and whether the adhesion process changes the structure of the liquid crystalline ordering of the lipid bilayer.

Based on the results obtained in the section 3.2, we observe a similar POPE multilayer structure for the data set presented in Fig. 6. The reflectivity curve from the thick coating results in a decrease in intensity at the critical edge. The thin coating was modeled as include 20-25 flat POPE bilayers leading to the appearance of the observed Bragg peaks. The final fitting parameters are listed in Table 2.

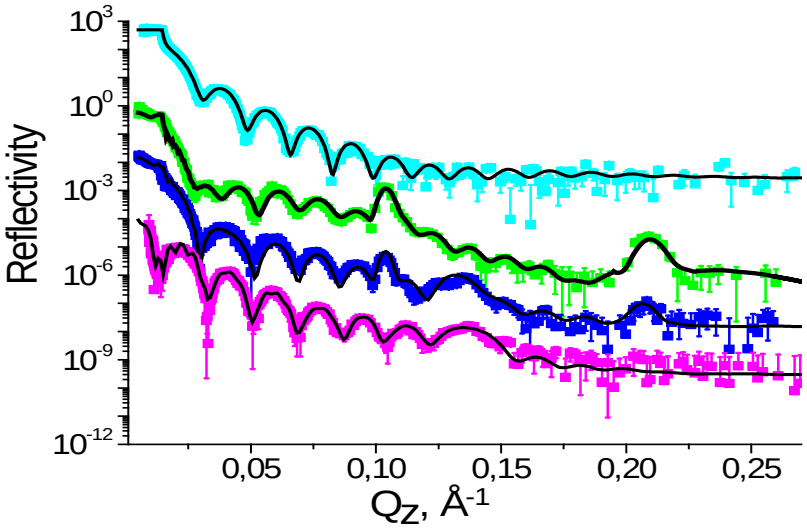

FIG. 6 Neutron specular reflectivity curves. The cyan curve corresponds to the Ti coated Si-crystal measured against D_2O. The green curve corresponds to the POPE coated substrate measured against D_2O. The blue curve corresponds to the POPE coated substrate measured against D_2O-based growth medium with deuterated HSA. The violet curve corresponds to the POPE+dHSA sample against H_2O. The black curves represent the fits to the measureddata. Curves are displayed with vertical offset for clarity.

Table 2. Neutron SLD profile of the POPE coated substrate at 20 °C in the presence of dHSA.

Sample	Material	Thickness, Å	SLD, 10^{-6} Å^{-2}	Roughness, Å
Ti coated Si-crystal	Si	None	2	None
	SiO_2	40	3.4	8
	Ti	368	-1.96	13
	TiO_2	25	2.4	15
POPE thin coating – the first multilayer structure				
Lipid Multilayer structure 25 repetitions	Water layer	6±2	1.3±1	5±3
	Head group	6±3	0.5±0.5	8±3
	Tail group	36.7±3	-0.3±0.5	15±6
	Head group	6±3	0.5±0.8	10±4
	Water layer	6±2	1.3±1	5±3
POPE-dHSA complex – the second multilayer structure				
8 repetitions	dHSA	23	4±0.8	7
	POPE lipid	24	2.5±0.8	7
POPE thick coating				
Smeared out POPE bilayers	Smeared out POPE bilayers	20,000±5000	4±1	8±3

Moreover, an additional broad Bragg peak can now be observed in the reflectivity curve for the POPE+dHSA sample, which corresponds to a second multilayer structure of approximately 8-10 repetitions with a d-spacing of 45.7 Å (see the blue curve in Fig. 6). The origin of the additional Bragg peak is due to the implementation of the protein into the lipid system that is confirmed by the contrast experiment carried out in H_2O based

growth medium with the addition of dHSA. As one can see from the violet curve in Fig 6, the Bragg peaks from POPE multilayer structures are not present anymore at this SLD contrast, which is almost matching the SLD value of the POPE hydrophobic tail. However, the peak remains at the position of about 0.134 $Å^{-1}$ demonstrating that the additional peak is associated with the addition of HSA to the system.

So far only the POPE multilayer structure in z direction, perpendicular to the metal surface, has been considered; however, it is possible to gain some important information about the in-plane structure as well. First of all, the POPE multilayer structure shows very strong off-specular scattering, the so-called Bragg sheets that is clearly visible in Fig. 7A and Fig. 7 D. The Bragg sheets (see Fig. 7A) are associated with the thick POPE coating. Our specular reflectivity analysis shows that the thick POPE coating has smeared out density profile in z direction, as it is shown in section 3.4. However, the off-specular signal reveals that the inter-bilayer correlation is extremely strong.

For the dHSA and POPE multilayer structure, weaker Bragg sheets are observed at Q_z = 0.136 $Å^{-1}$ (see Fig. 7D). Considering a cut shown in Fig. 7C along Q_x at Q_z = 0.136 $Å^{-1}$,it can clearly be seen that the intensity is much more concentrated around the specular reflection region with Q_x smaller than $2x10^{-4}$ $Å^{-1}$. Moreover, in contrast to the Bragg sheet from the POPE multilayer structure, the off-specular intensity is here comparable to the background level (see Fig. 7D). The shape of the Bragg sheet indicates that the second multilayer structure consists of well-defined layers. This in-plane structure is consistent with the in-plane structure of the thin POPE coating that is well oriented in z direction (weak out-of-plane fluctuations) and, thus, show no strong Bragg sheets. The consistence of these two in-plane structures could be an indirect indication that the second multilayer structure is related to a thin flat coating located between islands of thick rough coatings. A sketch of the refined model is given in Fig. 8.

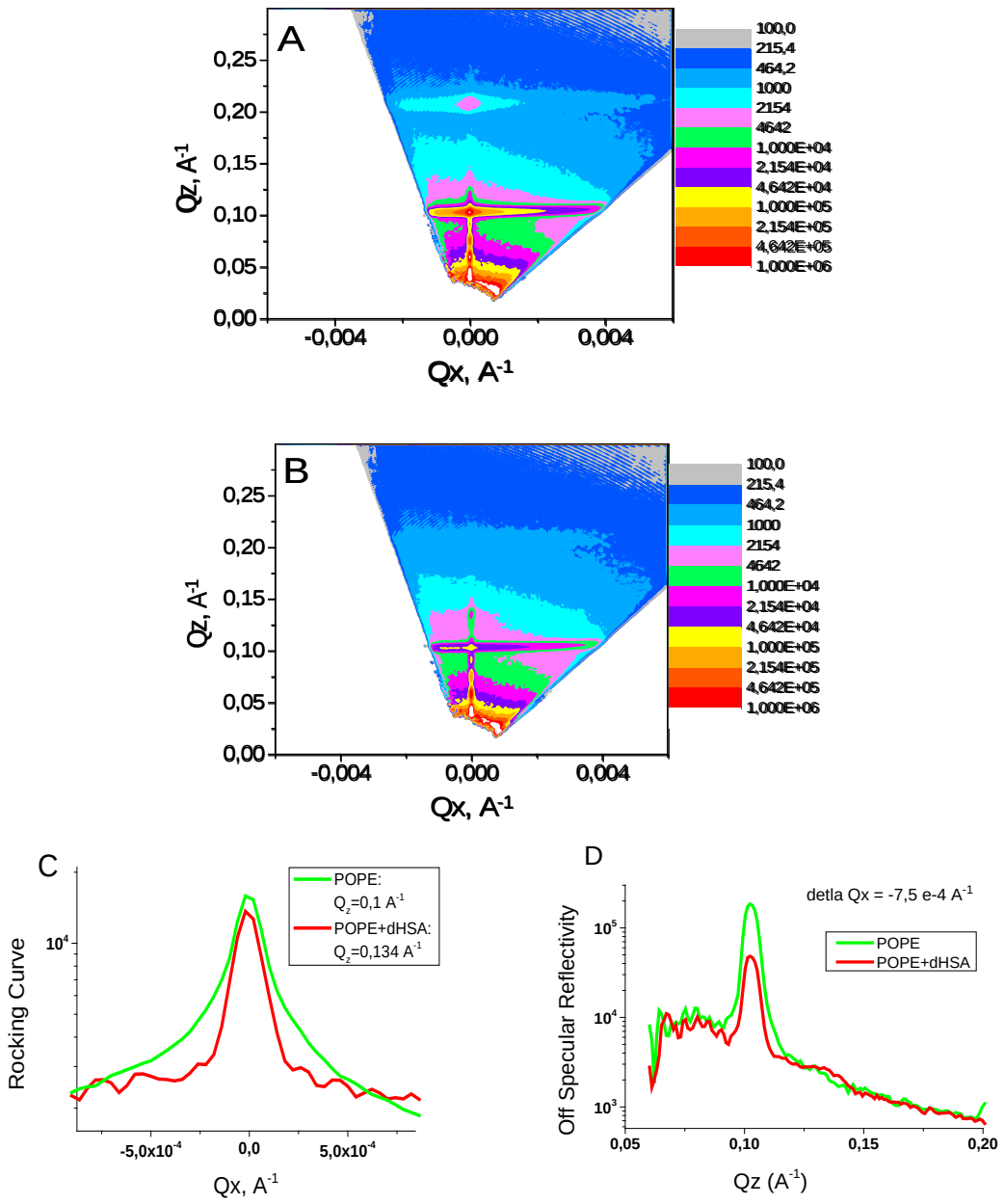

FIG. 7 Q maps – POPE lipid coating measured in D_2O (A) and in D_2O-based growth medium with deuterated HSA (B). The cuts over the Q maps are separately shown: C) green line corresponds to the cut of Q map A at Qz = 0.1 $Å^{-1}$ and red curve – the cut of the Q map (B) at Qz = 0.134 $Å^{-1}$, the rocking curves are rescaled for better view; D) Off specular cuts at Qx=-0.00075 $Å^{-1}$ – green line shows the cut over the Q map (A) and red curve – Q map (B).

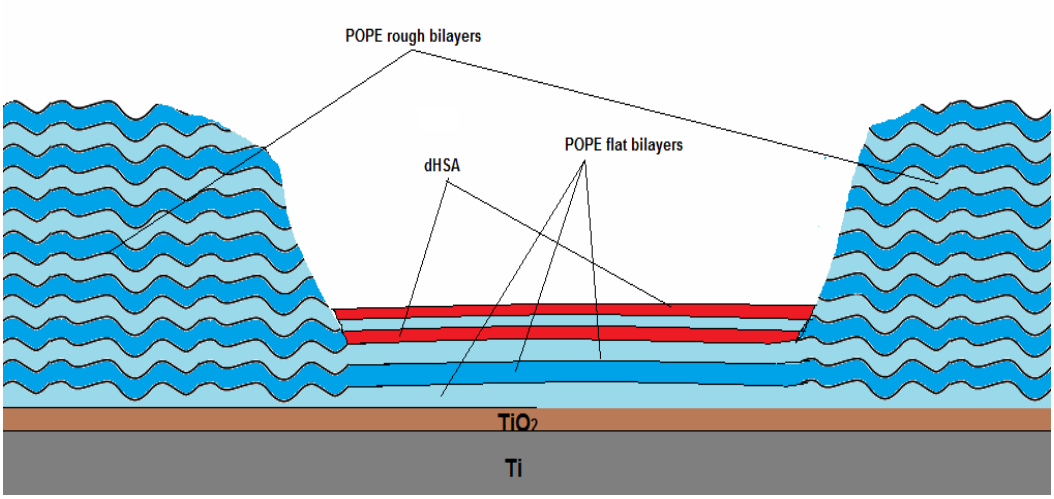

FIG. 8 Sketch of the POPE coated substrate in the presence of dHSA. The sketch presents the thick, not well ordered POPE coating and thin POPE coating together with the protein layers.

IV. DISCUSSIONS

The lipid deposition technique considered in this study was spray coating, which has the advantage that it is easier to handle and allows one to fully coat irregular surfaces with lipids. On the other hand, spray coating leads to less well defined lipid bilayers that potentially could lead to coating instability under wet conditions. For this reason, it has been considered a poor prospective deposition method in literature [32]. However, so far POPE lipids have not been deposited by the spray coating technique. We show by SEM measurements that the POPE spray coating led to two types of surface coatings. The first type contained 25-35 macroscopically flat POPE bilayers that coated approximately 60% of the titanium surface. The second coating was a 1-2 μm thick bulk-like system that covered up to 40% of the surface.

The crucial question here is whether the bilayers on top of the POPE coating are stable. This question might be difficult to answer by applying direct methods of investigation such as AFM and SEM, because in the case of a thick POPE coating some lipids remain at the surface even after the top bilayer is lost. Reflectivity experiments allow the total amount of POPE on the surface to be monitored. The drop in intensity at the critical edge of the measured reflectivity curve, for example, indicates a straightforward correlation between the thickness of the coating and the absorbed part of

the beam across the whole illuminated sample. The neutron reflectivity experiments clearly proved that an exposure to water affects the coating only by changing its lateral structure – the quantity of deposited POPE lipids remains constant even under wet conditions. This result indicates that the spray-coating method satisfies all the requirements for an implant modification technique, including stability and completeness.

The neutron reflectivity experiment also showed that the d-spacing of the POPE bilayer decays linearly with temperature after the phase transition temperature. This result is in agreement with previous X-ray diffraction experiments of Rappolt [33]; however, in contrast to our experiment, the POPE multilayer stack was not in contact with bulk liquid. It is known that such a linear behavior indicates that the POPE bilayer thickness changes are caused only by melting of the hydrocarbon region [34]. Our modeling revealed that the neutron reflectivity data for different temperatures can be successfully fitted just by varying the thickness of the tail group. The fact that POPE bilayers do not absorb additional water molecules as the temperature increases is a great advantage of POPE lipids compared to lipids with other types of head groups when applied as an implant modification. For example, the thickness of the water layer between PC (Phosphatidylcholine) bilayers increases with temperature. Thus, the undulation forces may overwhelm the van der Waals attraction at a certain temperature [34], allowing the PC bilayers to fluctuate freely without correlation to each other. Therefore, PC bilayers are not really stable in a liquid environment and are very sensitive to any physical stress.

As a main result from the analysis of the off-specular neutron data it can be concluded that the inter-bilayer interaction does not break down and the whole POPE multilayer system fluctuates as one unit independently from the level of POPE bilayer alignment and from the number of POPE bilayers. Such a high level of POPE bilayer organization, that can only be detected by scattering techniques, minimizes the possibility that the top bilayer of the multilayer structure is lost even when a high number of bilayers are present, in contrast to lipids with a PC head group.

At the same time, our experimental results reveal that the HSA protein can be successfully implemented onto the POPE multilayer structure and, thus, makes it possible to mimic the optimal conditions for bone cell culture while still providing a stable POPE multilayer structure.

V. CONCLUSIONS

Neutron reflectometry of fully hydrated lipid coatings on a titanium surface showed that lipid myltilayers can be deposited and that they are stable even under elevated temperature conditions. The study also revealed that two types of structures were produced: well ordered and macroscopically flat POPE bilayers contained 25-35 layers that coat approximately 60% of the titanium surface; and a less ordered and much thicker deposit which is 1-2 μm thick and coats up to 40% of the surface.

The results from neutron specular and off-specular reflectivity measurements clearly reveal the stability of the POPE spray coating in contact with water due to a strong inter-bilayer interaction that does not break down in the range of physiological temperatures. The strong inter-bilayer interaction and the resulting small inter-bilayer separation are shown from the very intensive Bragg sheet observed in all measured Q maps. With respect to the stability requirements of a biomimetic implant coating, it can be concluded that POPE may be one of the most appropriate lipids for successful implant modification.

ACKNOWLEDGMENTS

The authors would like to thank Prof. Trevor Forsyth from the DLab at ILL for the supplement of the deuturated Human Serum Albumin.

REFERENCES:

1. Bosco, R., et al., *Surface Engineering for Bon Implants: A Trend from Passive to Active Surfaces.* Coatings, 2012. **2**: p. 95-119.
2. Zethraeus, N., et al., *Cost-effectiveness of the treatment and prevention of osteoporosis.* Oseoposros. Int., 2007. **18**: p. 2-23.
3. Roach, H.I., et al., *Pathobiology of asteoarthritis: pathomechanisms and potential therapeutic targets.* Current Drug Targets, 2007. **8**(2): p. 271-282.
4. Barrere, F., et al., *Advanced biomaterials for skeletal tissues regeneration: Instructive and smart functions.* Mater. Sci. Eng. Rep., 2008. **59**: p. 38-71.
5. Williams, D.F., *On the mechanism of biocompatibility.* Biomaterials, 2008. **29**: p. 2941-2953.
6. Tengvall, P. and Lunstrom, I., *Physico-chemical consideration of titanium as biomaterial.* Clin. Mater, 1992. **9**: p. 115-134.

7. Donlan, R.M. and Costerton, J.W., *Biofilms: Survival mechanisms of clinically relevant microorganisms.* Clinical Microbiology Reviews, 2002. **15**(2): p. 167-168.

8. Willumeit, R., et al., *Phospholipids as implant coatings.* J. Mater. Sci: Mater. Med., 2007. **18**(2): p. 367-380.

9. Sandrini, E., et al., *In vitro assessment of the osteointegrative potential of a novel multiphase anodic spark deposition coating for orthopaedic and dental implants.* Journal of Biomedical Materials Research Part B-Applied Biomaterials, 2005. **73B**(2): p. 392-399.

10. Bosetti, M., et al., *Cell behaviour on phospholipids-coated surfaces.* Journal of Materials Science-Materials in Medicine, 2007. **18**(4): p. 611-617.

11. Merolli, A. and Santin, M., *Role of Phosphatidyl-Serine in Bone Repair and Its Technological Exploitation.* Molecules, 2009. **14**(12): p. 5367-5381.

12. Willumeit, R., et al., *In-vitro interactions of human chondrocytes and mesenchymal stem cells, and of mouse macrophages with phospholipid-covered metallic implant materials.* European Cells and Materials, 2007. **13**: p. 11-25.

13. Luthringer, B., et al., *Production, characterisation, and cytocompatibility of porous titanium-based particulate scaffolds.* Journal of Materials Science-Materials in Medicine, 2013. **24**(10): p. 2337-2358.

14. Deing, A., et al., *A Porous TiAl6V4 Implant Material for Medical Application.* Int J Biomater, 2014. **2014**: p. 904230.

15. Luthringer, B., et. al., *Phosphatidylethanolamine biomimetic coating increases mesenchymal stem cell osteoblastogenesis.* J Mater Sci Mater Med, 2014. **25**(11): p. 2561-71.

16. Carter, D.C., et al., *Three-Dimension Structure of Human Serum Albumin.* Science, 1989. **244**.

17. Lee, L.T., et.al, *Neutron reflectivity of an oil-water interface.* Phys Rev Lett, 1991. **67**(19): p. 2678-2681.

18. Bhattacharya, A.A., et.al, *Crystallographic Analysis Reveals Common Modes of Binding of Medium and Long-Chan Fatty Acids to Human Serum Albumin.* J. Mol. Biol., 2000. **303**(5): p. 721-732.

19. Salditt, T., *Thermal Fluctuation and Stability of Solid-Supported Lipid Membranes.* Journal of Physics: Condensed Matter, 2005. **17**: p. R287-R314.

20. Salditt, T., *Lipid-Peptide Interaction in Oriented Bilayers Probed by Interface-Sensitive Scattering Methods.* Current Opinion in Stuctural Biology, 2003. **13**: p. 1-12.

21. Stoermer, M., et.al, *Structure and Corrosion of Magnetron Sputtered PUre Mg Film on Silicn Substrates.* Plasma Processes and Polymers, 2007. **4**(1): p. 557-561.

22. Golub, M., et al., *X-ray and neutron investigation of self-assembled lipid layers on a titanium surface.* Biointerphases, 2013. **8**.

23. Campbell, R.A., et al., *Figaro: The New Horizontal Neutron Reflectometer at the ILL*. The European Physical Journal Plus, 2011. **126**(107).

24. Holden, D.A., et.al, *Resistive-pulse detection of multilamellar liposomes.* Langmuir, 2012. **28**(19): p. 7572-7.

25. Zhai, Y., et al., *Physical properties of archaeal tetraether lipid membranes as revealed by differential scanning and pressure perturbation calorimetry, molecular acoustics, and neutron reflectometry: effects of pressure and cell growth temperature.* Langmuir, 2012. **28**(11): p. 5211-7.

26. Constantin, D., et al., *Solid-supported lipid multilayers: structure factor and fluctuations.* Eur Phys J E Soft Matter, 2003. **12**(2): p. 283-90.

27. Nelson, A., *Co-Refinement of Multiple-Contrast Neruton/X-ray reflctvity data using MOTOFIT*. Journal of Applied Crystallography, 2006. **39**: p. 273-276.

28. Parratt, L.G., *Surface Studies of Solids by Total Reflection of X-Rays.* Phys. Rev. Lett, 1954. **95**(2): p. 359-369.

29. Zabel, H., *X-Ray and Neutron Reflectivity Analysis of Thin Films and Superlattices.* Applied Physics A, 1994. **58**: p. 159-168.

30. Zarbakhsh, A., et.al, *A New Approach for Measuring Neutron Reflection from a Liquid/Liquid Interface.* Meas. Sci. Technol., 1999. **10**: p. 738-743.

31. Daillant, J., *X-ray and Neutron Reflectivity: Principles and Applications.* Lecture Notes in Physisc. Vol. 58. 1999.

32. Kreuzer, M., *Solid-Supportde Lipid Membranes and Their Response to Varied Environmental Conditions*. 2011, Institut für Weiche Materie und Funktionale Materialien F-I2.

33. Rappolt, M., et.al., *Structure and Elasticity of Phospholipid Bilayers in the Lα phase: a Comparison of Phosphatilylcholine and Phosphatidylethanolamine Membrane.* Recent Research Developments in Biophiscs, 2004. **3**: p. 363-392.

34. Lipowsky, R. and S. Leibler, *Unbinding Transitions of Interacting Memranes.* Phys. Rev. Lett, 1986. **56**: p. 2541-2544.